SR TOC

Proceedings of OMAE'02
21st International Conference on Offshore Mechanics
and Artic Engineering
June 23-28, 2002,Oslo, Norway

OMAE2002-28409

# RISK-BASED INSPECTION PLANNING FOR MOORING CHAIN

Jan Mathisen
Det Norske Veritas, Høvik, Norway

Kjell Larsen
Statoil, Trondheim, Norway

## ABSTRACT

The use of risk-based inspection planning for offshore structural components is becoming quite familiar. This paper describes an application of this technique to mooring chain. In many cases, the technique is based on probabilistic modelling of fatigue crack growth in the structural components, and updating of the failure probability on the basis of inspections. The extension of this basis from a single component to very many components is necessary to tackle series systems, such as mooring chain, where a fatigue fracture can arise in any chain link. The theoretical basis for the analysis is described, including details of the model for stochastic dependency between the chain links. Results are shown that compare failure probabilities for a single chain link and a chain segment. The effects of various levels of inspection coverage are illustrated.

An example of a cost optimal inspection plan is developed for mooring chain on an FPSO in the northern North Sea.

Keywords: inspection planning, mooring lines, fracture mechanics, structural reliability.

## INTRODUCTION

### Background

Permanently moored floating structures for oil and gas production are widely used worldwide today. Mooring chain with its long application experience and good abrasion characteristics is still the most important mooring component. However, the industry has experienced several chain failures over the years. Most of these failures can be related to degradation through crack growth. Due to the increasing use of chain as important permanent load bearing components, with a design lifetime up to 30 years, it is evident that good control of the long-term condition of these elements is crucial for the structural safety of the floating structure.

One strategy for condition control of permanently installed mooring lines may be divided into six separate activities:

1. Annual underwater inspection by use of ROV.
2. Periodic winch maintenance.
3. Periodically changing the chain links in contact with the fairlead by operational winching.
4. Annual measurement of chain link diameter of the links in the splash zone.
5. Annual assessment of mooring line loads and accumulated fatigue damage by evaluation of vessel motions and available mooring line tension measurements.
6. Periodic control of the upper chain segments by non-destructive testing (NDT), using magnetic particle inspection (MPI) onshore. This requires on-site change out of segments and transportation to shore using anchor handling tugs; an operation which is quite costly.

This paper addresses the requirement for NDT control based on use of MPI (activity 6). An approach using risk-based inspection (RBI) planning methods for systematic condition control and cost optimization is assessed and described. The main challenges in the analysis are to provide a realistic model for probabilistic crack-growth in a single chain link, and to take a large number of chain links into account, with a realistic correlation between links. The result of the analysis is a plan stating when it is cost-optimal to inspect the chain. Some results are shown for chain from a turret-moored ship in Norwegian waters. The uppermost chain segment in the most heavily loaded mooring line is considered. This chain has been conservatively designed, with a fatigue safety factor of 10. The present example is intended to illustrate the method without providing full details of the case study.

### Previous Work

Reliability analysis of mooring lines in the DEEPMOOR joint industry project (ref. Mathisen, 1999a) forms some of the background for the present work. Considerable experience was gained in analysis of ultimate, accidental and fatigue limit states, and in using these results to calibrate the design rules for mooring lines, presented by Okkenhaug (2001). Although inspection methods for mooring lines were not addressed in this project, it seemed that they were empirically based, and might benefit from systematic analysis. At the same time, risk-based inspection planning has been applied to jackets, semisubmersibles, and floating production systems, as described by Sigurdsson et al. (2000). The present work describes a first attempt to apply risk-based inspection planning to mooring chain.

## METHOD

### Fatigue Loading

The fatigue loading of mooring chain is generally taken to be due to the tension cycles induced in the chain by;

- low-frequency platform motions in a horizontal plane, due to wind gusts and 2nd order wave loads, and
- wave-frequency motion of the platform with 6 degrees of freedom due to 1st order wave loads.

The magnitude of the tension cycles is also dependent on the mean tension in the line, due to pretension and mean environmental loads.

Standard methods are available to compute the fatigue damage due to these tension cycles under the Miner-Palmgren hypothesis, as described in DNV's OS-E301, or API RP 2SK. In the present case, intermediate results from the fatigue analysis made during the mooring line design are used to establish a long-term distribution of tension ranges. A Weibull distribution function is fitted to this data. This distribution function may be written

$$F_P(\Delta p) = 1 - \exp\left\{-\left(\frac{\Delta p}{a}\right)^b\right\} \qquad (1)$$

where $\Delta p$ is the magnitude of a tension range (peak to trough), $a$ is the scale and $b$ is the shape parameter of the distribution. It applies to the most heavily-loaded mooring line, and effectively includes both low-frequency and wave-frequency effects, with a mean period of 14 s in the case study.

### Crack Growth Model for Chain Fatigue

#### Crack growth

Cracks are assumed to grow from the surface of a chain link, with a semi-elliptical shape, as indicated in Fig. 1, where $a$ is the crack depth and (lower case) $c$ is half the crack length.

The crack growth is modelled by linear fracture mechanics, using the Paris-Erdogan equation in the 2-dimensional form:

$$\frac{da}{dN} = C(\Delta K_A)^m; \quad \Delta K_A > \Delta K_{th} \quad ; \quad a(N_0) = a_0 \qquad (2)$$

$$\frac{dc}{dN} = C(\Delta K_C)^m; \quad \Delta K_C > \Delta K_{th} \quad ; \quad c(N_0) = c_0 \qquad (3)$$

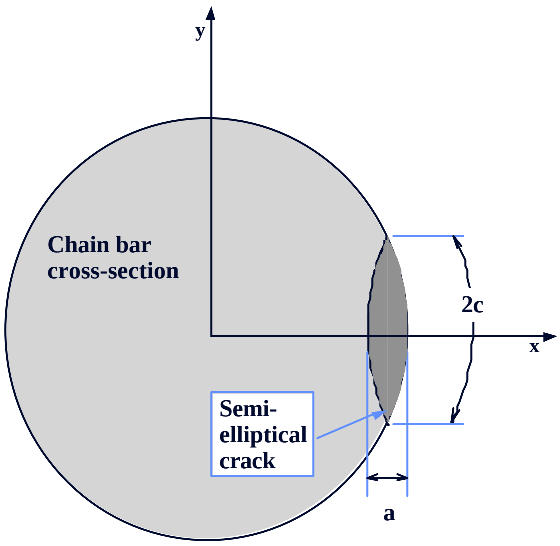


**Figure 1 Crack size.**

These equations provide the increment in the crack depth and crack half-length from one tension cycle, where $N$ represents the number of tension cycles. The subscripts, $A$ and $C$, refer to the deepest point of the crack, and to an end point of the crack at the surface, respectively. $m$ and (upper case) $C$ are material parameters, and are taken from BS7910. $\Delta K_A$ and $\Delta K_C$ are applied stress intensity ranges at the two locations indicated by the subscripts. $\Delta K_{th}$ is a stress intensity threshold, below which no crack growth takes place. This threshold is not applied in the present analysis; i.e. it is effectively zero. $a(N_0)$ indicates the initial crack depth before any load cycles have been applied; i.e. at $N = N_0$, and $c(N_0)$ indicates the initial half-length of the crack.

A finite element analysis has been carried out to determine the local stresses due to the applied tension, in an intact, studless, chain link. The stress distributions have been established for 3 cross-sections located at the weld, in the bend, and at the crown of the link. A sample stress distribution is shown in Figure 2. Standard practice in crack growth analysis, based on BS7910, is to linearise the actual stress distribution using a combination of membrane and bending stress components, as indicated in Figure 3.

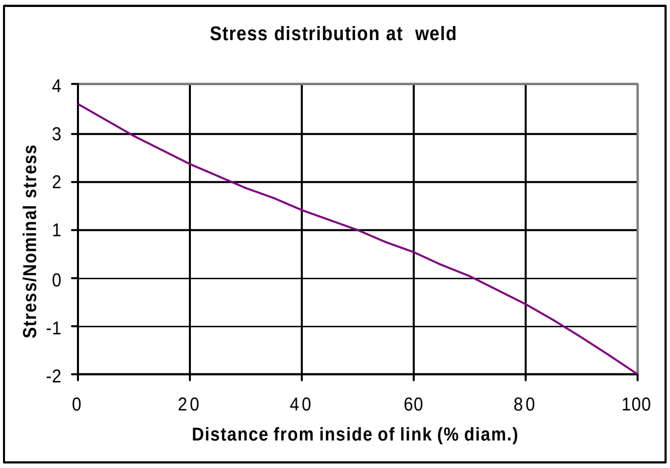


**Figure 2 Stress distribution over a cross-section through weld for an intact, studless link.**

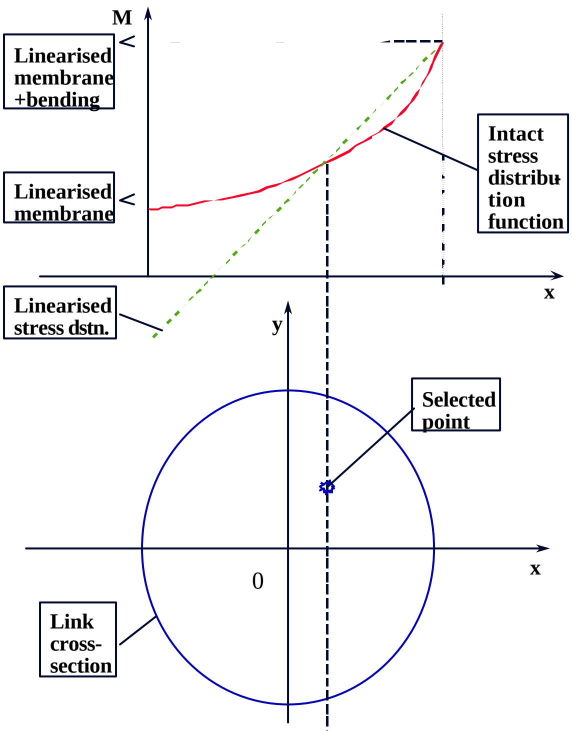


**Figure 3 Linearisation of stress distribution over a selected cross-section through an intact link.**

The stress intensity ranges applied in equations (2) and (3) are taken as the sums of the stress intensity ranges due to membrane (subscript *m*) and bending (subscript *b*) stresses. The stress intensity range for either membrane or bending stress is obtained by

$$\Delta K_{ij} = \Delta s_{\,j}(x) \cdot Y_{ij}(a,c) \cdot \sqrt{pa}\ , \quad i = A, C, \quad j = m, b \qquad (4)$$

where index $i=A$ indicates the crack tip at the deepest point and index $i=C$ is for the crack tip on the surface, index $j=m$ indicates membrane stress and index $j=b$ is for bending stress, $\Delta s$ is a stress range, and *Y(a,c)* is a geometry function that takes account of the effect of the presence of the crack on the stress distribution. In the present analysis, we are assuming that the crack propagates symmetrically with respect to the x-axis in Figure 3. This implies the same crack growth at both ends of the crack on the surface, and that the deepest point of the crack lies on the x-axis. Cracks may start from defects away from the x-axis, but will tend to align themselves in this way as they grow larger, according to Pommier et al. (1999).

Numerical geometry functions developed by Klasen and Dillstrom (2001) are applied in the present analysis. Their results have been extended down to infinitesimal crack size using results from Pommier et al. (1999). An example is given in Figure 4, showing good agreement with a collection of data for this type of geometry functions by Coroneau (1998).

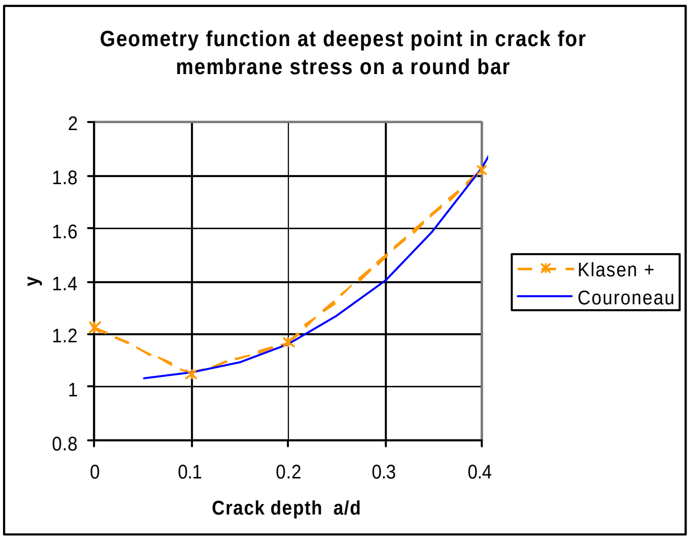


**Figure 4 Example of geometry function (for a straight flaw), compared to Couroneau (1998).**

## Critical crack depth

The link is defined to fail when the crack depth reaches the critical crack depth. The critical crack depth is calculated as the crack depth that will just lead to rupture when the line tension level corresponds to a return period of 1 year. This line tension is obtained from the original design analysis of the mooring system. A level 2A failure assessment diagram (FAD) from BS7910 is used to calculate the critical crack size. The fracture toughness of the link material is needed for the FAD, and is obtained from the Charpy V impact tests carried out during the production of the chain links. The yield strength and ultimate tensile strength are also taken from the chain production test data. The following critical crack depths are obtained:

12% of chain diameter at weld section,
30% of chain diameter at bend section,

15% of chain diameter at crown section.

The weld section has the lowest fracture toughness, while the outer part of the crown section has the highest nominal tensile stress level .

The initial condition of the chain is assumed to be as it is immediately after production, corresponding to the test links that are used in S-N tests. The mean value of the initial crack size in the crack growth model is deterministically calibrated to provide the same time to failure as given by S-N analysis, using the logarithmic mean value of the K-parameter of the S-N curve. This parameter is taken from an S-N curve that Mathisen et al. (1999b) have fitted to data including some results from the joint industry study on Studless Chain Fatigue, organised by Noble Denton and Associates Inc., with testing by the National Engineering Laboratory. These data apply specifically to R4 grade studless chain in a salt water environment. The linear fracture mechanics model does not normally include the crack initiation phase. With this calibration method, the crack initiation phase is inserted in the model by applying very small initial crack sizes. Furthermore, consistency with this calibration principle implies consideration of a single crack location in each chain link. The weld section is chosen for the crack location in this analysis.

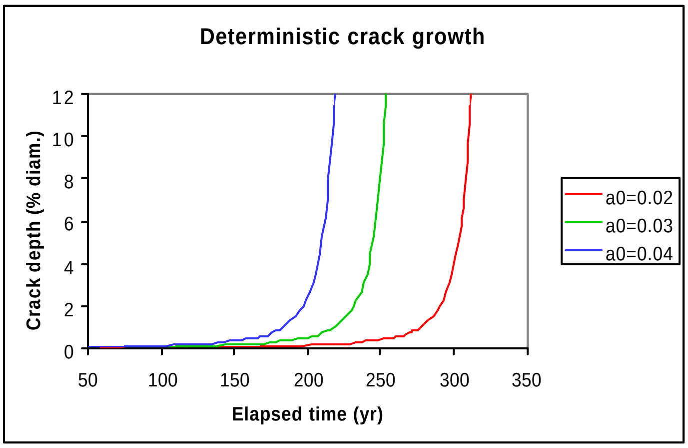


**Figure 5 Deterministic crack growth with initial crack depths 0.02, 0.03, 0.04 mm.**

Examples of deterministic crack growth curves are shown in Figure 5 and Figure 6, obtained by integrating equations (2) and (3) with fairly representative parameters. The time to critical crack size is long, but is sensitive to variation in the initial crack size. The crack initiation phase is long, followed by relatively rapid crack growth. The case in Figure 6 shows a crack size that might be detected if the link were inspected during the 30 year interval before critical crack size.

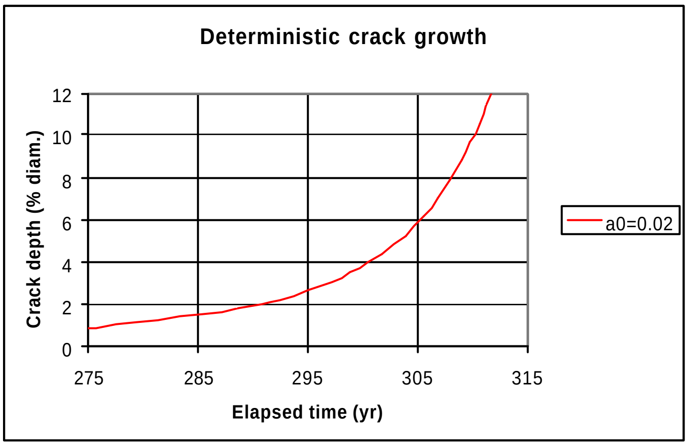


**Figure 6 Latter part of deterministic crack growth with initial crack depth 0.02 mm.**

## Reliability Analysis of a Single Link

The link survival event $E_S\left(t;\mathbf{Q},\mathbf{R}_{x[1]}\right)$ is defined to occur if the crack depth is less than the critical crack depth at time $t$. The following random input variables are included in the analysis:

- $Q_1$ the scale parameter of the Weibull distribution of tension ranges, used to model load model uncertainty, with a normal distribution and 15% coefficient of variation (CoV),
- $Q_2, R_{X2}$ the variability in the material parameter, as a normal variable, with CoV based on BS7910,
- $Q_3, R_{X3}$ the model uncertainty in the geometry function, as a normal variable with 5% CoV,
- $R_{X1}$ the initial crack depth, with exponential distribution,
- $R_{X4}$ the aspect ratio of the initial crack $a_0/c_0$ , as a normal variable with 10% CoV.

The global random vector $\mathbf{Q}$ includes components which are common to all links, while the local random vector $\mathbf{R}$ includes components which are independent between links. The variability in the material parameter $C$ and in the geometry function is split evenly between global and local parts. The distinction between global and local variables is not important for a single link, but is essential for the treatment of many links. The symbol $x$ is included to allow for subsequent distinction between two groups of links, $x$ and $y$, while the subscript $[1]$ on the local random variable indicates the number of links and the corresponding number of independent, identically distributed occurrences of this variable. The accumulated probability of failure up to time $t$ is given by the complement of the survival event The annual probability of failure is taken as the difference in the accumulated probability over the year that is considered.

### Reliability Analysis of a Chain Segment

The chain segment survival event $E_S\left(t;\mathbf{Q},\mathbf{R}_{x[m]}\right)$ is defined to occur if the crack sizes in all the $m$ links in the segment are less than the critical crack size at time $t$. It is essential to provide an appropriate level of stochastic dependency between the individual links in order to obtain meaningful reliability results for the chain segment. This is often referred to as correlation between the links. The present approach is introduced above in the definition of the link failure event. The difference between link and segment survival events lies in the number of instances of the local random vector $\mathbf{R}_{x[m]}$.

Since, the same tension is experienced by the whole chain segment (to a good approximation), the load model uncertainty is taken to be a global variable. The initial crack depth and aspect ratio are taken to be local variables. The material parameter $C$ and the uncertainty in the geometry function are both split into global and local parts, with half the original variance in each part.

This segment model is based on judgement and some experience. It would be desirable to have a better basis in empirical data for the modelling of the dependency between the links. It turns out that the variability of the initial crack size is a dominant effect in the present analysis, as might be expected from Figure 5, so that the independence of this variable between links is a key assumption. The local variability in material parameter is also important, while the local uncertainty in geometry function appears to be less important.

The reliability calculation is nested in two layers, where the inner layer handles a conditional probability, conditioned with respect to the global variables. Integration over the probability distribution of the local variables takes place in the inner layer. Integration over the probability distribution of the global variables is carried out in the outer layer. The number of links are taken into account between these two steps. The first order reliability method (FORM) is applied in the reliability calculations, using the PROBAN program (Sesam, 1996).

## Inspection

### Inspection and Repair Procedure

The chain segment is inspected ashore, after being replaced by a spare segment. Magnetic particle inspection (MPI) is applied. Only a sample of the links in the chain are normally inspected by MPI. 5% of the links are generally inspected, with 100% inspection in some parts, such as chain on windlasses or fairlead. Crack indications are often found on initial inspection. If these crack indications disappear after very light surface grinding then they are disregarded, as being due to inadequate surface preparation. Further grinding may be applied to repair cracks, to a maximum depth of 7% of the chain diameter. Larger cracks are repaired by replacing the chain link or the entire chain segment. The dimensions of detected cracks are not normally measured. The present chain segment has been inspected once after 3 years in service, without any cracks being detected.

### Inspection Accuracy

The accuracy of the inspection technique is defined in terms of a probability of detection (PoD) curve. A PoD curve for common Nordic industrial practice, taken from Førli (2000), is assumed to be applicable. The curve is shown in Figure 7. The original curve provides a small probability of detecting very small defects, that is unrealistic, but usually of no importance. The present application is sensitive to this approximation, because the inspection is applied many times – to a large number of links. A lower limit has been introduced to the curve at 0.3 mm defect depth to reduce this sensitivity.

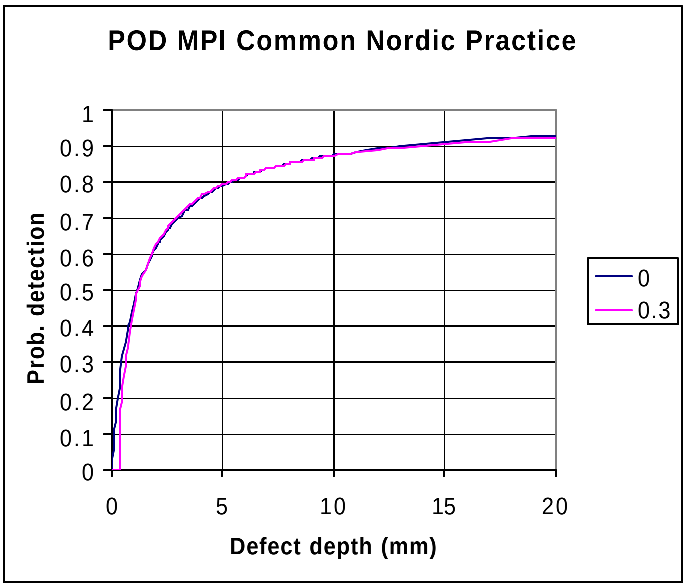


**Figure 7 Probability of detection curve, with lower limits for defect depth of 0 and 0.3 mm.**

### Reliability Updating for One Chain Link from Inspection

Let us denote the event of no detected crack in one link, from inspection at time $t_i$, by $E_I\left(t_i;\mathbf{Q},\mathbf{R}_{x[1]},\mathbf{D}_{x[1]}\right)$. This event implies that the crack size at inspection time is less than the detectable crack size $\mathbf{D}_{x[1]}$, where the latter is a random variable with distribution defined by the PoD curve. Again, the subscript is designed to indicate inspection of a single link from link group $x$.

The probability of survival can then be updated by expressing it as a conditional probability, which is computed from the probability of the intersection of the 2 events (both survival and inspection events take place), divided by the probability of the conditioning event

$$P\left[E_S(t;\mathbf{Q},\mathbf{R}_{x[1]})\middle|E_I(t_i;\mathbf{Q},\mathbf{R}_{x[1]},\mathbf{D}_{x[1]})\right] = \frac{P\left[E_S(t;\mathbf{Q},\mathbf{R}_{x[1]})\bigcap E_I(t_i;\mathbf{Q},\mathbf{R}_{x[1]},\mathbf{D}_{x[1]})\right]}{P\left[E_I(t_i;\mathbf{Q},\mathbf{R}_{x[1]},\mathbf{D}_{x[1]})\right]} \quad (5)$$

This type of reasoning can be extended to include several inspections at different times, by including additional inspection events.

## Reliability Updating for a Chain Segment from Inspection

The probability of chain segment survival can also be updated from inspection results, by extension of the expression in equation (5). In principle, the number of events considered has to be extended to include the failure events for all links, and the no-find events for all links that are inspected. Let us specify that group $x$ contains all $m$ links which are inspected, while group $y$ contains all $n$ links which are not inspected, and that groups $x$ and $y$ together include all the $m+n$ links in the segment. Then the conditional probability of survival of the segment is given by

$$P\left[E_S(t;\mathbf{Q},\mathbf{R}_{x[m]})\bigcap E_S(t;\mathbf{Q},\mathbf{R}_{y[n]})\middle|E_I(t_i;\mathbf{Q},\mathbf{R}_{x[m]},\mathbf{D}_{x[m]})\right] = \frac{P\left[E_S(t;\mathbf{Q},\mathbf{R}_{x[m]})\bigcap E_S(t;\mathbf{Q},\mathbf{R}_{y[n]})\bigcap E_I(t_i;\mathbf{Q},\mathbf{R}_{x[m]},\mathbf{D}_{x[m]})\right]}{P\left[E_I(t_i;\mathbf{Q},\mathbf{R}_{x[m]},\mathbf{D}_{x[m]})\right]} \quad (6)$$

where $\mathbf{D}_{x[m]}$ represents $m$ independent instances of the detectable crack size. Care has to be taken to insure that each link is treated consistently, so that the same stochastic variables are considered for failure and inspection events of that link. The present notation is designed for this purpose. It is convenient to formulate in terms of the complementary events of link survival rather than link failure, since the survival event for the chain segment is provided by the intersection of survival events for all the links.

Only the no-find event is considered from inspections in the present analysis. This is the most likely type of event for a chain which is conservatively dimensioned with respect to fatigue. The other, most relevant, inspection event would be that a crack has been detected – a find event. Find events can, in principle, occur at any inspection, and in any number of inspected links. It is impractical to consider all possible combinations of no-find and find events when developing an inspection plan early in the life of a mooring system. However, if cracks are found later, then the inspection plan can be revised on the basis of these events.

Typical practice is to select every 20th link for inspection, with more frequent inspection in some zones. Hence, there is probably some tendency to inspect the same links in repeated inspections. However, this is not guaranteed. It is impractical to take account of which links are inspected in reliability analysis of multiple inspections. It should be conservative to assume that the same links are inspected each time, since this implies less control of the possibility for failure in the other links.

## Costs

Typical inspection costs are expected to lie in the range from MNOK 4 to MNOK 8. These costs are dominated by hire costs for a chain handling vessel, to retrieve the chain segment for inspection, and insert the replacement segment. The cost of the actual MPI is a marginal part of the inspection cost.

Repair costs are not relevant because only no-find events are taken into account from the inspections. Simple grinding repairs of occasional, small cracks would not add any significant cost.

The cost of a single line failure is estimated to be about 20 MNOK. This includes the cost of a replacement chain segment, installation of this segment, and the expected cost of lost production due to a reduced production window while one line is missing. Hence the ratio between single line failure cost and inspection cost lies in the range from 2.5 to 5.

If mooring system failure cost is considered, then the cost ratio may be as much as 3500. Mooring system failure is not usually expected to be a probable consequence of a single fatigue failure. However, if the initial rupture of a link with a fatigue crack occurs in severe weather, and a neighbouring line is about as highly utilised in fatigue, then rupture of a fatigued link in that neighbouring line may follow. This situation may lead to mooring system failure, if the weather is severe enough.

A discount rate of 6% p.a. is applied in the cost analysis.

## Optimisation

The analysis is based on a cost optimisation, including:

- inspection cost,
- failure risk cost.

Repair cost is negligible in the present case.

A number of trial inspection plans are formulated, and the total costs are computed for each plan. The cost-optimal plan is found by selecting the trial plan that leads to the lowest costs. Each trial inspection plan is set up for a different target probability level, and inspections are applied when the probability of failure exceeds the target level.

Each inspection plan is considered in turn. The inspection cost is a simple deterministic function of the trial inspection plan. The updated probability of mooring line failure is also predicted, assuming that no cracks are detected at the planned inspections. The failure risk cost is taken as the costs associated with the fatigue failure of one mooring line, multiplied by the probability of failure.

## RESULTS

### Single Link

The probability of failure of a single link is shown in Figure 8. This is the basic reliability calculation and form of presentation in the present paper, so it may be worthwhile to include some detailed comments. The time axis shows the elapsed time in years since the chain entered service. The probability axis shows the probability of failure, where failure is defined as a crack growth exceeding the critical crack depth at the weld location in the chain link. A logarithmic axis is applied to the probability. Most of the curves show the accumulated probability of failure over all elapsed years from the start of service. In some cases the annual probability of failure is also shown, as the increase in accumulated probability of failure during the last year.

The probability of link failure is very small initially, and increases gradually with time. Note that there is no allowance for surface defects introduced in the transportation, installation, or operation of the chain in these results. The annual probability of failure of a single link is quite low, even at the end of the design life.

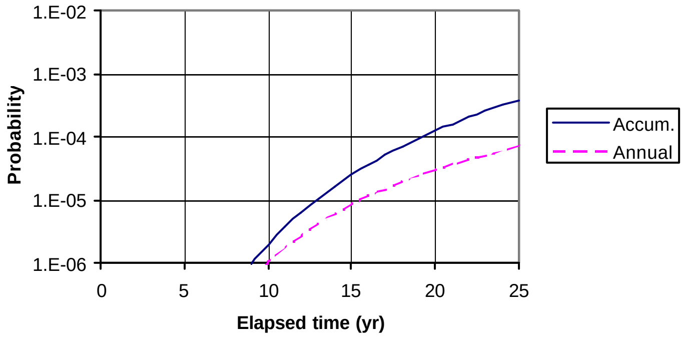


**Figure 8 Probability of failure of a single link**

Some conditional probability results are shown in Figure 9, showing how inspection with no crack found reduces the probability of failure. The probability of failure is reduced immediately after the inspection, but the effect of the inspection decreases as the time after the inspection continues to increase. Some reasons for the effect of the inspection can perhaps be explained as follows:

- Our initial knowledge of the fatigue behaviour of the chain link is based on a rather general capacity distribution, which usually implies considerable uncertainty. Inspection of the link with no defect found indicates that some of the more unfavourable possibilities contained in the capacity distribution are not realised in the present link.
- Furthermore, since no defect is detected, the crack growth model indicates that failure of the link is improbable in the near future.

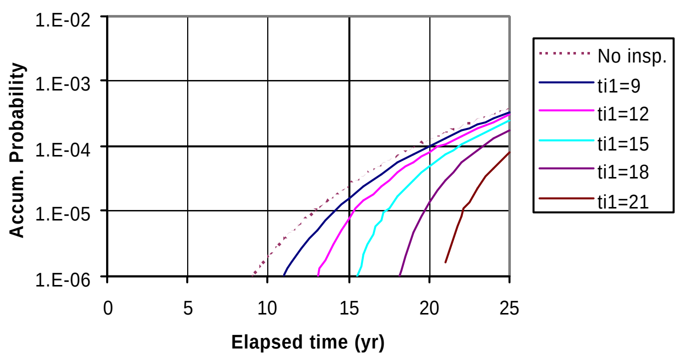


**Figure 9 Probability of failure of a single link, conditional on inspection with no crack detected, at time ti1.**

### Chain Segment

The top chain segment has 154 links under tension between the fairlead and the adjacent wire rope segment. The basic result for the probability of failure of the segment is shown in Figure 10. Due to a conservative fatigue design, there is only an accumulated probability of failure of 0.02 by the end of the design life – fatigue failure is fairly unlikely, but not highly improbable. The annual probability of failure at the end of the design life is $4 \times 10^{-3}$.

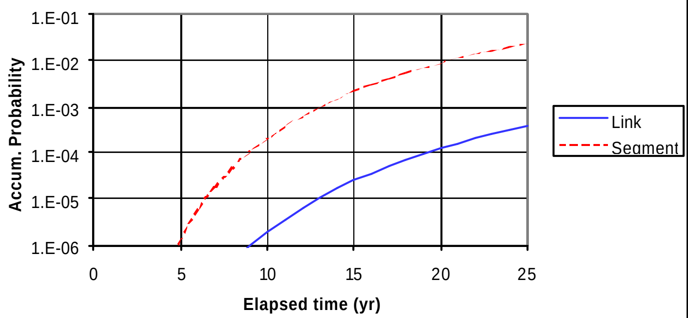


**Figure 10 Comparison of accumulated probability of failure for a single link and a chain segment.**

A comparison of link and segment probabilities of failure is also shown in this figure. The segment is 61 times more likely to have failed than the link by the end of the design life. This ratio is a consequence of the correlation between links that is implicit in the present analysis model. It shows that the correlation is low. Since the correlation is low, it follows that inspection of one link does not yield a confident assessment of the condition of another link. Furthermore, there is a relatively small number of chain links in the present chain segment, and the increase in cost of inspecting all the links is marginal. On this basis, it was decided to base the inspection plan on MPI of each individual link.

 

## Inspection

A large number of parameter studies on the effects of inspection are needed for the optimisation of an inspection plan. A few examples are shown in this section. It is assumed that all the links in the chain segment are inspected at each inspection, and that no cracks are found in any links. The probability of failure is given conditional on these inspection events, based on generalisation of the expression in equation (5).

The effect of a single inspection on the probability of failure of the chain segment is shown in Figure 11, for inspections after 5, 10, 15 or 20 years. The uppermost curve in this figure shows the probability of failure with no inspection. The probability of failure is significantly reduced after an inspection with no-finds. In subsequent years, the probability of failure tends to increase, and gradually approach the curve for no inspections. Results of this type are developed for a single inspection in all years from year 3 to year 25.

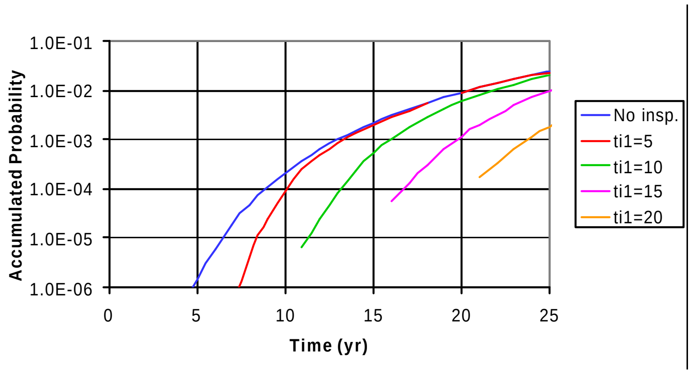


**Figure 11 The effect of one inspection, with no-finds in all links, on the probability of failure, for inspections after 5, 10, 15, or 20 years.**

The effect of two inspections is shown in Figure 12. The 1st inspection is in year 13 and the 2nd inspection in any year from year 14 to year 17. The same general effect is seen for the 2nd inspection as for the first inspection. There is a little irregularity in some of the curves for the second inspection, in the 1st year or two after the inspection. This is due to numerical difficulties in computing these problems more accurately. Fortunately, the general trend is very regular, and these curves can be faired manually by comparison with adjacent curves, if necessary. The curves are also manually extrapolated back to the year of inspection, for use in the inspection planning. Similar results are computed for 2nd inspections in every year between initial inspections and the end of the design life.

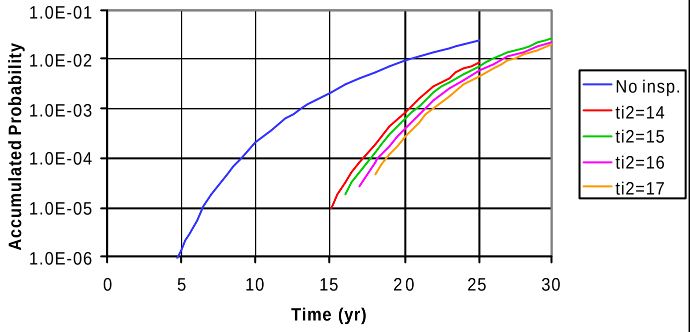


**Figure 12 The effect of two inspections, with no-finds in all links, on the probability of failure, for the second inspection after 14, 15, 16, or 17 years, with the first inspection after 13 years.**

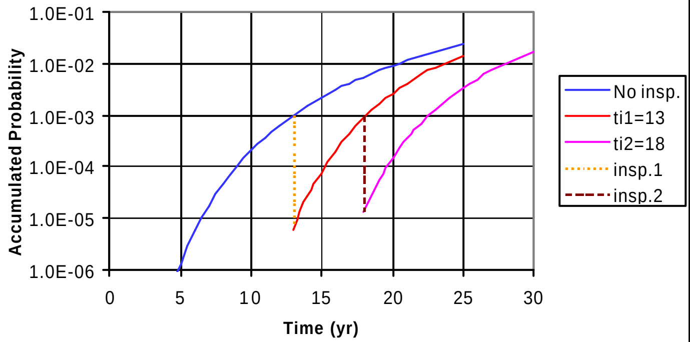


**Figure 13 Illustration of part of an inspection plan with a target probability of $10^{-3}$.**

Figure 13 shows how these results may be utilised in establishing an inspection plan. In this example, a target probability of failure of $10^{-3}$ is selected to determine the plan. The curve for the probability of failure with no inspections is followed until this target probability is exceeded, after 13 years. The first inspection is applied then. Provided no cracks are detected, the probability of failure drops, and the curve for one inspection at 13 years is followed, until the target probability is again exceeded, after 18 years. A second inspection is then applied. Again, provided no cracks are detected, the probability of failure drops, and the curve for a second inspection at 18 years is followed until the target is exceeded after about 23 years. A 3rd inspection would be applied then, but this is not shown on the figure.

The target probability is an accumulated probability in this example, but an annual probability is often applied instead. The application of a target probability in this way is an effective way of controlling the risk cost of failure; i.e. the probability of failure multiplied by the cost of failure.

## Optimisation

When the cost ratio of failure cost to inspection cost is 2.5, then it is cost-optimal to omit in-service inspections of the chain, in the present case study. This remains the case up to a cost ratio of about 90. The cost elements for this case are shown in Figure 14. The minimum cost is still found at target Pf=0.1, at which no inspections are required, but the failure risk cost now exceeds the inspection cost at this target.

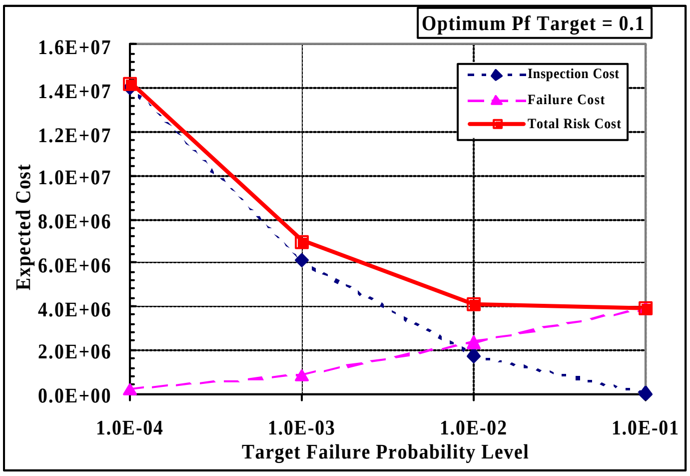


**Figure 14 Cost elements plotted against target level for failure to inspection cost ratio of 90.**

When the cost ratio is increased to 120, the optimal target is Pf=0.01, as shown in Figure 15. Now, one inspection is cost-optimal, after 21 years, as shown in Figure 16.

When the cost ratio is increased further to 1500, then the optimal target is Pf=0.0001, as shown in Figure 17. Now, six inspections are cost-optimal, with the first after 9 years, as shown in Figure 18.

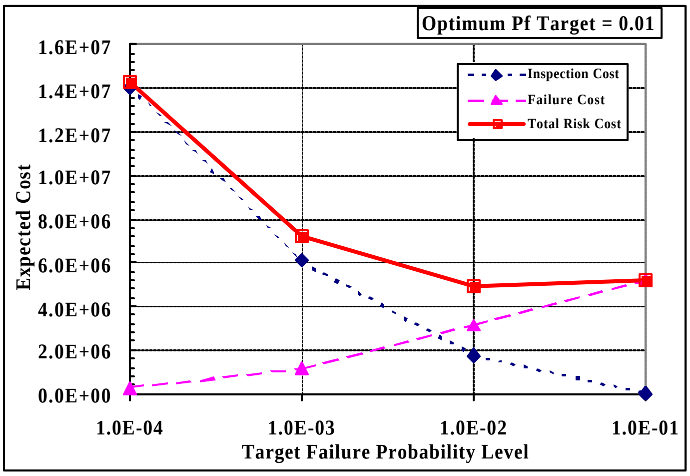


**Figure 15 Cost elements plotted against target level for failure to inspection cost ratio of 120.**

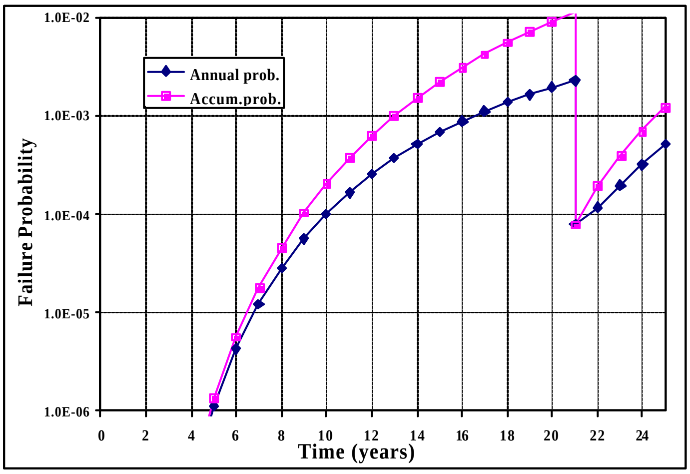


**Figure 16 Updated failure probability with cost-optimal inspection plan for failure to inspection cost ratio of 120.**

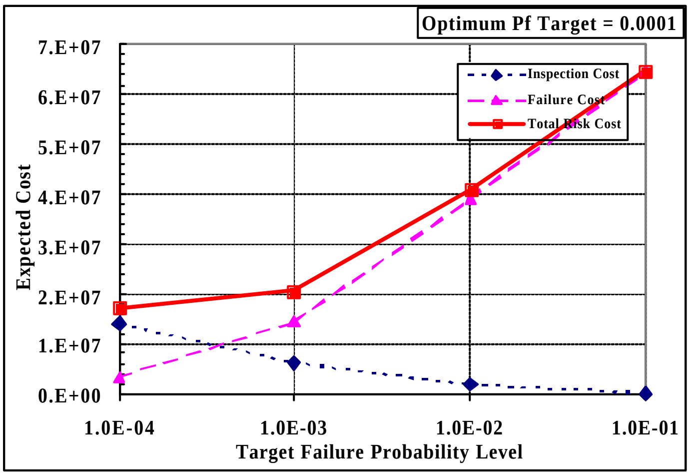


**Figure 17 Cost elements plotted against target level for failure to inspection cost ratio of 1500.**

## CONCLUSION

A fatigue reliability analysis of a studless chain link has been developed on the basis of linear fracture mechanics, and calibrated against S-N data for this type of chain, in a saltwater environment. The reliability analysis has been extended from a single link to a chain segment, while taking account of the stochastic dependency (or correlation) between the chain links. Probabilistic updating of the fatigue reliability on the basis of results from chain inspections has been carried out, by comparing the predicted crack sizes with an appropriate probability of detection curve for magnetic particle inspection. A systematic series of reliability analyses have been made, with and without updating for inspection. These results have been combined with the cost of inspection and the risk cost of failure to derive a cost-optimal inspection plan.

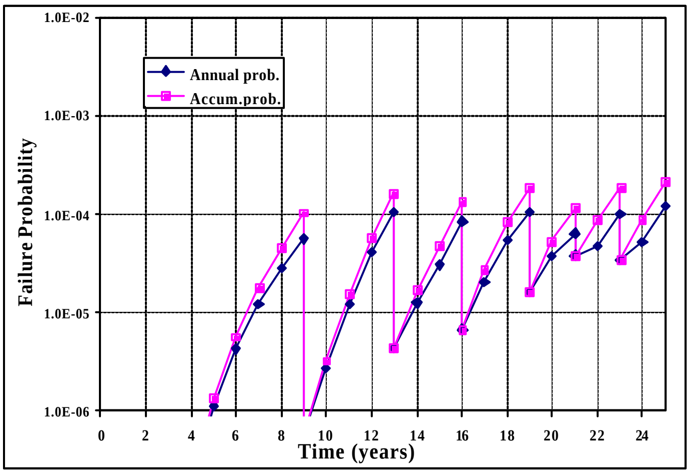


**Figure 18 Updated failure probability with cost-optimal inspection plan for failure to inspection cost ratio of 1500.**

In the present case study on a rather short and conservatively designed chain segment:

- it has been found to be preferable to inspect all links rather than the usual sample of links, if inspection is carried out,
- it is found to be cost-optimal to omit in-service inspections if a single line failure in fatigue does not lead to further line failures.

Note that the present analysis only addresses fatigue failure of chain due to normal cyclic loading. It does not take account of the effects of sub-standard chain quality or accidental damage to the chain. The model can be used to investigate the sensitivity of the results to some effects of this type, but they cannot be fully incorporated in the analysis because they are not adequately quantified. An initial inspection during installation, or early in the service life is usually good practice, to guard against such effects. Regular visual inspection of the chain may also be advisable. Furthermore, an accidental limit state is included the design basis to ensure that the mooring system is designed with an allowance for line failures due to such effects.

A single mooring line failure is not normally expected to cause significant risk to the safety of personnel, or significant risk of pollution. This is not necessarily the case for mooring system failure. If there are significant risks of these types, then safety requirements usually take precedence over cost-optimal considerations. Hence, it may be useful to quantify the risk of a single line failure escalating to a mooring system failure. The particular scenario involved here implies that empirical statistics may not be suitable for this purpose, since a change in inspection procedure is involved, which tends to invalidate empirical data based on standard inspection procedures.

## ACKNOWLEDGMENTS

This application of risk-based inspection planning to mooring lines was originally suggested as a joint industry project, but failed to gain a sufficient number of sponsors. It has now been carried out on behalf of Statoil. Permission to publish this work is gratefully acknowledged. The material presented herein should not necessarily be taken to represent the views of Statoil or of DNV. Note also that some input data have been changed to separate the results presented here from the actual ship that was originally analysed. Cooperation from Statoil colleagues, Petter Nyborg, Sigvald Kleppe and Per Terje Wold, and DNV colleagues, Bjørn Klasen, Agnar Karlsen and Gudfinnur Sigurdsson, is also gratefully acknowledged.

## REFERENCES

API, (1995), “Recommended Practice for Design and Analysis of Stationkeeping Systems for Floating Structures,” RP2SK, American Petroleum Institute, Washington D.C.

BSI (1999), “Guide on methods for assessing the acceptability of flaws in fusion welded structures,” BS 7910, British Standards Institution.

Det Norske Veritas, (2001), “Offshore Standard DNV-OS-E301, Position Mooring,” Høvik.

Couroneau, N., Royer, J., (1998), “Simplified model for the fatigue growth analysis of surface cracks in round bars under mode I,” Int. Journal of Fatigue, Vol.20, no. 10, pp.711-718.

Førli, O., (2000), “RBI for Offshore Structures – Service Development, POD curves for electromagnetic NDT,” memo no. forl/00aaabx1, DNV Materials Technology and Laboratories RN530, Høvik.

Klasén,B., Dillstrøm,P, (2001), private communication of results from stress analysis of a bar with flaws of various sizes.

Mathisen, J., (1999a), “Changes to DNV’s POSMOOR Rules, Based on the DEEPMOOR Project,” Seminar on Dynamic Positioning and Mooring of Floating Offshore Structures, Norwegian Soc. of Chartered Engineers, Sandefjord.

Mathisen, J., Hørte,T., Moe,V., Lian,W., (1999b), “DEEPMOOR – Design Methods for Deep water Mooring Systems, Calibration of a Fatigue Limit State,” Det Norske Veritas, report no. 98-3110, rev.no. 03, Høvik.

Pommier, S., Sakae, C., Murakami, Y., (1999), “An empirical stress intensity factor set of equations for a semi-elliptical crack in a semi-infinite body subjected to a polynomial stress distribution,” Int. Journal of fatigue, Vol.21, pp.243-251.

Okkenhaug, S., (2001), “DNV POSMOOR – New Edition 2001,” conference on Dynamic Positioning and Mooring of Floating Offshore Structures, Norwegian Society of Chartered Engineers, Kristiansand.

SESAM, (1996), “User’s Manual PROBAN General Purpose Probabilistic Analysis Program,” DNV Software report no. 92-7049, rev.no. 1, Høvik.

Sigurdsson, G., Lotsberg, I. & Landet, E., (2000), “Risk Based Inspection of FPSOs”, Int. Conf. on Offshore Mechanics and Arctic Engineering, OMAE'2000, New Orleans.

 